Transmission anomalies in Kerr media photonic crystal circuits: Intrinsic localized modes

Arthur R. McGurn*
Department of Physics, Western Michigan University, Kalamazoo, Michigan 49008, USA

Gulay Birkok
Gehze Institute of Technology, Department of Physics, P.O. Box 141, 41400 Gebze-Kocaeli, Turkey
(Received 22 May 2003; revised manuscript received 12 January 2004; published 14 June 2004)

A study is made of the exact solutions of a system of nonlinear difference equations that model the propagation of electromagnetic radiation in photonic crystal waveguides and networks of interconnecting photonic crystal waveguides (photonic crystal circuits) containing Kerr nonlinear dielectric media. The transmission properties of a waveguide formed of linear dielectric material and containing a barrier of Kerr nonlinear material are determined and shown to exhibit anomalies similar to those due to gap solitons in layered Kerr nonlinear optical media. Similar discussions for a nonlinear segment bisected by a waveguide composed of linear dielectric media are given. The transmission properties of a junction formed from Kerr nonlinear media connecting three semi-infinite waveguides formed from linear dielectric materials are also determined. The transmission of electromagnetic energy through the junction is found to exhibit anomalies similar to those due to gap solitons in layered Kerr nonlinear media. The transmission anomalies in the systems we study are shown to arise from intrinsic localized modes that are found in the Kerr nonlinear media of the system. Intrinsic localized modes are solitonlike modes that can only exist in nonlinear systems. Previous transmission studies presented by us have concentrated on systems formed of linear media, and no previous transmission studies have been presented by us on systems supporting intrinsic localized modes. The central focus of this paper and new results presented are the study of resonant transmission anomalies in photonic crystal circuits containing Kerr media and the identification of some of these resonances with intrinsic localized modes that exist is the Kerr media.

DOI: 10.1103/PhysRevB.69.235105 PACS number(s): 42.70.Qs, 42.81.Dp, 05.45.Yv

I. INTRODUCTION

Recently there has been much interest in photonic crystal waveguides and circuits in two-dimensional photonic crystals.[1–14] The photonic crystal is a periodic array of cylinders of linear dielectric media with axes that are arranged on a two-dimensional lattice [see Fig. 1(a)]. Waveguides and networks of interconnecting waveguides are introduced into the photonic crystal by replacing some of its cylinders by cylinders containing impurity dielectric materials. The impurity cylinders are spaced at equal intervals along a row of the photonic crystal, forming waveguide channels which in turn can be interconnected to make circuits. The theory of these structures, for channels composed of linear dielectric media has been worked out in detail,[5–7] and more recently some discussions of the existence of intrinsic localized modes (ILM) in channels formed from Kerr nonlinear media have been put forth.[8–14] The ILM are solitonlike modes that can only exist in nonlinear media. The present paper is concerned with these more recent discussions on ILM in Kerr nonlinear systems, presenting a theoretical discussion on how ILM could be observed experimentally using the transmission properties of photonic crystal circuits composed of linear dielectric media and containing arrays of nonlinear sites formed from Kerr nonlinear dielectric media. (These systems differ from previously studied Kerr systems which were composed entirely of Kerr nonlinear media.) In this Introduction we briefly review the method of difference equations used by us to treat the electromagnetic field distributions and transmission properties of photonic crystal waveguides and circuits. This is followed by some remarks as to where current work on photonic crystal waveguide and circuit systems that support ILM stands. Finally, an outline of the theory to be presented in this paper is given (including a summary of ideas of resonant spectroscopy) as an overview of the calculations found in the text. The central focus of this paper and new results presented are the study of resonant transmission anomalies in photonic crystal circuits containing Kerr media and the identification of some of these resonances with ILM that exist in the Kerr media.

It has been shown that under certain circumstances the electromagnetic modes in photonic crystal waveguides and circuits are obtained as the solutions of a set of difference equations.[5–14] These equations relate the electromagnetic fields within each of the impurity cylinders forming the channels to one another. The solutions of the difference equations give the channel fields for a wide variety of propagating and localized modes bound to the waveguide and circuit channels. Knowing the channel fields, the fields throughout all space are obtained by evaluating an integral equation[5–11] and the transmission properties of propagating wave solutions are determined.

The difference equation approach describes the physics of waveguides and circuits in terms of the solutions to a system of equations that are easy to solve and that are similar to those arising in the study of other physical phenomena.[15–25] For linear dielectric waveguides the difference equations are isomorphic to those describing excitations in phonon and magnon systems. The solutions are propagating waves and exponential states.[5–11] For Kerr nonlinear dielectric

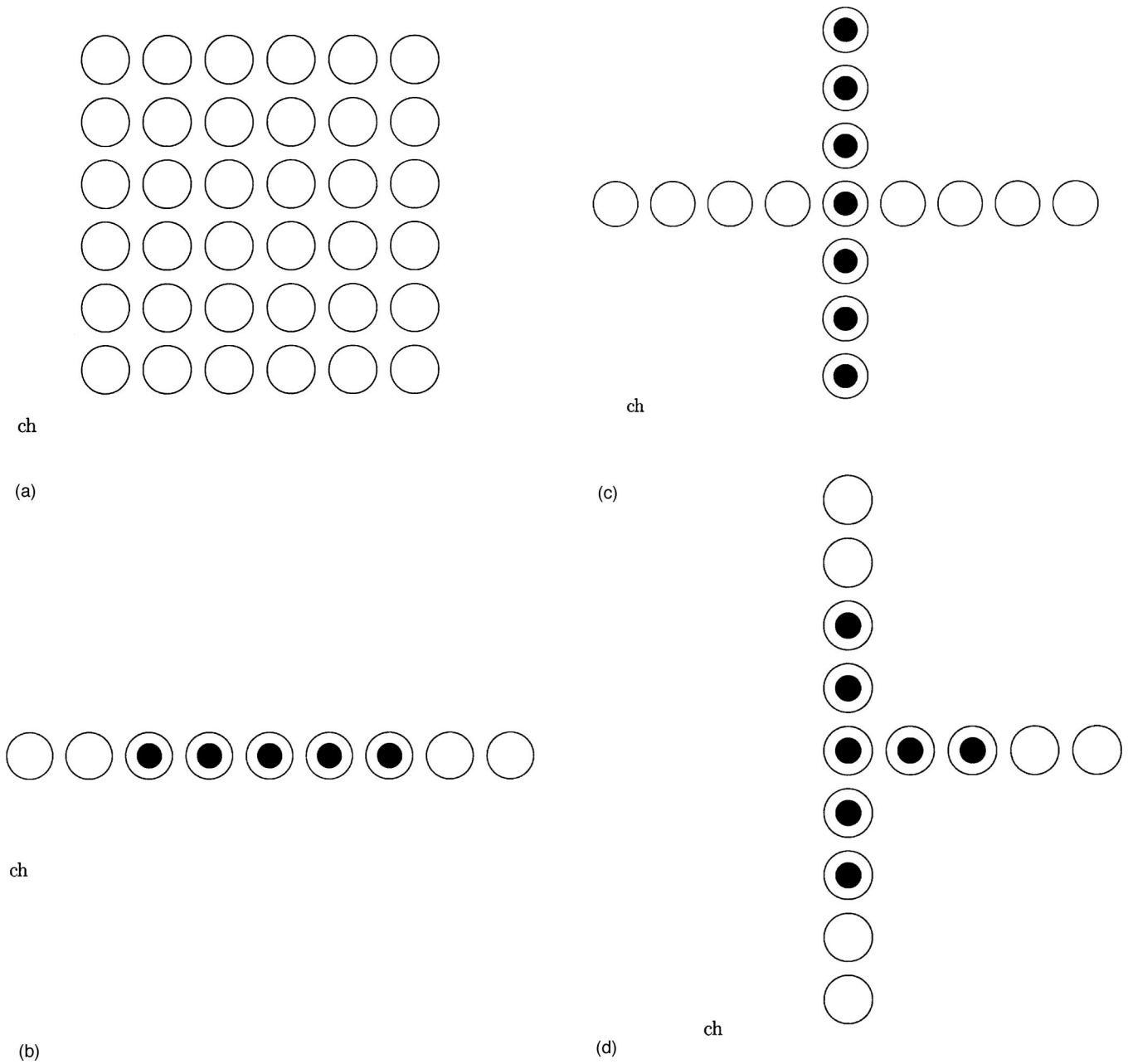

FIG. 1. (a) Schematic drawing of square lattice photonic crystal. The cylinders are of dielectric constant ϵ_0 and are embedded in vacuum. The axes of the cylinders are parallel to the z-direction (perpendicular to the page) and are ordered in the $x-y$ plane (page) on a square lattice. (b) Schematic drawing of a waveguide channel with a barrier. Only the photonic crystal cylinders forming the channel are shown. The cylinders of linear material are open and the cylinders of nonlinear material have filled centers. (c) Schematic drawing of an infinite waveguide of linear media that perpendicularly bisects a Kerr segment. Only the photonic crystal cylinders forming the waveguides are shown. The cylinders of linear material are open and the cylinders of nonlinear material have filled centers. (d) Schematic drawing of a finite waveguide junction connecting linear waveguide channels. Only the photonic crystal cylinders forming the waveguide and junction channels are shown. The cylinders of linear material are open and the cylinders of nonlinear material have filled centers.

waveguides the difference equations are isomorphic to those encountered in the study of intrinsic localized modes (ILM) in the vibrational properties of chains of atoms with nonlinear interatomic interactions.[8–10,15–25] This means that, under the proper conditions, ILM exist in photonic crystal waveguides and circuits made from Kerr nonlinear media. Due to the isomorphism that exists in the difference equation method between photonic crystal systems and nonlinear vibrational systems, the difference equation theory offers a natural approach to the study of ILM in photonic crystal circuits containing Kerr nonlinear media.

Recently, as indicated above, a number of theoretical treatments have been presented discussing the conditions needed for ILM to exist in photonic crystal waveguides and circuits made entirely from Kerr materials.[8–14] (See Ref. 25 for a detailed review of this work.) The focus of the theory

presented in this paper is to advance these discussions to consider how ILM could be observed experimentally in linear dielectric photonic crystal waveguides and photonic crystal circuits that contain barriers, segments, and junctions of Kerr nonlinear media. It is suggested that ILM could be observed in anomalies found in the transmission of electromagnetic energy through these types of systems. (This introduces a new aspect to our treatment of the transmission characteristics of photonic crystal waveguides and circuits as our previous work focused on the transmission properties of systems formed from linear dielectric media. The transmission properties of systems containing Kerr nonlinear media that supported ILM were not addressed by us in our previous work.) A number of transmission anomalies are found in the nonlinear systems treated in this paper, and these anomalies are shown to be directly related to ILM that only exist in the Kerr nonlinearity of the materials forming the barrier or junction scattering sites. The anomalies observed are similar to (but not the same as) those associated with gap solitons in layered nonlinear optical media.[26–28] The ILM are a general property of the nonlinear difference equations of the waveguides, and the results given here can be generalized to systems described by similar sets of nonlinear difference equations, i.e., phonon, magnon, and other systems treated by tight-binding Hamiltonian formulations. An interesting aspect of the photonic crystal circuits is that they exhibit ILM transmission anomalies in systems of higher topological dimension than that of layered optical media.[25–28]

The method of study used in our discussions of ILM transmission anomalies in Kerr nonlinear photonic crystal circuits is similar to that used by Chen and Mills[28] in the study of gap soliton transmission anomalies in Kerr nonlinear layered optical media. The systems treated by Chen and Mills, however, are quite different than ours and the soliton modes studied by Chen and Mills are quite different from the ILM (solitonlike modes) studied by us. In this paper, the transmission through and electromagnetic fields in a photonic crystal circuit containing Kerr nonlinear media is solved exactly. Transmission coefficient and field distribution plots are generated numerically from these solutions. (The formulas of the exact solutions are very large and messy so they are not listed here. A systematic way for generating the formulae of the exact solution is given in the text.) Transmission anomalies are identified in the numerical data. The exact electromagnetic field distribution in the Kerr media at the transmission anomalies is determined from the exact solutions. Approximate solutions for the ILM electromagnetic fields in infinitely long Kerr nonlinear waveguides and photonic crystal circuits made completely of Kerr nonlinear media (from Refs. 7 and 8) are then matched with the exact field distributions of the systems treated in this paper at the transmission anomalies. In this way the transmission anomalies are determined to be due to ILM in the barriers, segments, and junctions.

In this approach, the resonant transmission is explained as a type of hopping phenomenon. The fields incident from a waveguide of linear dielectric media onto the Kerr nonlinear barrier tunnel to the resonantly excited ILM in the barrier and then tunnel from the ILM in the barrier to transmitted waves in the waveguide of linear media on the other side of the barrier. Without the assistance of the ILM intermediate state the transition across the barrier would be much less probable and the transmission resonance would not be present.

An alternative rationale can be given for the transmission method used by Chen and Mills in their study of gap solitons and adopted here in our treatment of intrinsic localized modes. In physics a variety of different types of resonant scattering phenomena are observed. The resonances treated by Chen and Mills and by us are closely related to one of these types as described by a text that is commonly used at many universities. In Sec. 1.4 of the text by Friedrich[29] certain types of resonances that occur in atomic scattering are discussed. In referring to these resonances Friedrich states that "Resonances appear [when] $\cdots$ a slight modification of the Hamiltonian would lead to a bound state." Because the state is not quite bound in the system its lifetime is long (this gives rise to the resonant cross section) but not infinite (as per a real bound state). Our system is not an atomic physics system, but we think that the same principle is applicable. Consider the nonlinear layered media systems of Chen and Mills and our nonlinear photonic crystal waveguide systems. In the limit that these are of infinite extent, it is demonstrated that solitons and ILM exist in these two systems. Next make a slight modification to these infinite systems. This is done by locating a soliton or ILM and modifying the systems in the regions surrounding these modes. Go to a distance far from and on either side of the the peak in the mode electromagnetic field distribution and cut off the ends of the nonlinear media. Finally, replace the cut off nonlinear media of the old ends of the system by new ends formed from linear optical media, e.g., let the Kerr nonlinearity be zero in the two end regions. Only the portion of the nonlinear systems containing the bulk of the highly localized field distributions of the soliton and ILM is retained. Since the field distribution of the modes is small in the parts of the systems that have been changed, these changes should be small perturbations on the modes. The excitations which were formerly bound solitons and ILM should now be states of long but finite lifetimes. They are resonant states that can couple to incident, transmitted, and reflected waves in the linear media attached to the sides of the nonlinear Kerr segments. The presence of the formerly bound soliton and ILM should show up as resonant anomalies in the transmission coefficients of the nonlinear segments for conditions under which the infinite nonlinear systems would support solitons or ILM, respectively. This is then another way of viewing the increased transmission effects caused by the presence of the soliton or ILM whose presence in the barrier facilitates resonant tunneling.

Resonant scattering occurs in a variety of phenomena observed in atomic, solid state, nuclear, and high energy physics. Closely related to our barrier transmission problems are transmission resonances in electronic tunnel junctions and Josephson junctions. Resonances can be observed in electronic tunnel junctions when electrons tunneling through the junctions interact with spins, atoms and molecules, or even lattice vibrations in the non conducting junction materials.[30,31] Such resonant interactions show up as anomalies in the current voltage characteristics of the junction, and

these are essentially transmission anomalies. The Josephson effect may be regarded as a resonant transmission anomaly. The observation of most of these effects is through the determination of the current (transmission) characteristics as a function of potential (energy or frequency) and this is the property generally used to fix the resonance. In the work of Chen and Mills and here, as added proof of the resonant scattering, the wave function within the barrier is presented in addition to the transmission properties. This is to satisfy the reader that not only does a resonance exist at the frequency, dielectric constants, and Kerr parameters that we would expect to see a soliton or ILM mode resonance, but for this parametrization the barrier material supports a field distribution that is very close to that of the soliton or ILM in the infinite systems where these, respectively, exist as bound states. In this paper we also show that off-tuning the system from the ILM resonance conditions not only stops the transmission resonance, but off resonance the fields in the Kerr barrier are on longer distributed in the form of an ILM and the maximum field intensity in the barrier is greatly reduced from its value at resonance. It is not unreasonable to us that these criterion are sufficient to classify the anomalies presented in Chen and Mills and in this paper as transmission resonances arising from ILM. As a final note, we point out that optical resonance transmission properties have recently been applied to the study of excitonic resonances in two-dimensional photonic crystal slabs.[32] The transmission of light is found in these studies to be affected by coupling to excitons in the slab. These resonances are of a different type than those treated by Chen and Mills and by us here, but the use of resonance transmission ideas is similar.

ILM modes have only recently been observed in some non optical experimental systems[25–33] and these have been one-dimensional. Some work on optical systems has very recently appeared as discussed in the "note" following this paragraph. Photonic crystal waveguides and circuits would be good candidates for the observation of optical ILM. In addition, due to the branchings and interconnecting nature of photonic crystal circuits, these systems would be good for the study of ILM in more topologically complex systems than simple linear chains systems.

(Note: Since this paper was originally submitted for publication some experiments on ILM in parallel waveguide arrays have been made and presented in Physical Review Letters.[34] The geometry and propagation characteristics of light in these systems is quite different from those studied here by us. In addition, many months after our original submission a feature article has appeared in Physics Today dealing with the experimental observation of intrinsic localized modes in a variety of discrete nonlinear system,[35] including some optical systems different than those considered here by us. Our present paper focuses on proposing a method for the observation of intrinsic localized modes in photonic crystal circuits. These are a type of discrete nonlinear system. We refer the reader to the Physics Today article of Ref. 35 for a detailed review of experiments already done on other type of discrete nonlinear systems including other optical systems.)

II. WAVEGUIDE EQUATIONS

Consider a square lattice photonic crystal formed from linear dielectric media and its electromagnetic modes with electric fields polarized parallel to the axes of the cylindrical dielectric rods of the photonic crystal [see Fig. 1(a)]. The photonic crystal lattice constant is a_c, the radii of the dielectric cylinders is R, and the lattice sites in the $x-y$ plane at which the cylinder axes are located are labeled by integers (n,m) in the usual manner.[5,6,8,9] The axes of the cylinders are parallel to the z-direction.

A waveguide is formed in the photonic crystal by replacing a straight line array of cylinders with cylinders containing impurity dielectric media.[1–14] The replacement cylinders are equally spaced and their closest separation may be further than nearest-neighbor along the direction of the waveguide channels, e.g., the closest separation between adjacent replacement cylinders may be second or third or etc. neighbor along the channel direction.[5–9,25] If the electric field inside the impurity material of any given impurity cylinder forming the channel can be approximated as a constant over the impurity material of that cylinder (see Refs. 5–11 and 25 for a discussion of this point), then the modes of the waveguide are described by a set of difference equations. (A similar set of difference equations is generated in a treatment of photonic crystal waveguides based on the so called coupled resonator optical waveguide model.[12,13]) The general form of the difference equations for such a straight waveguide of slope s/r in the $x-y$ plane made from Kerr nonlinear media is then[8]

$$E_{nr,ns} = \gamma[\alpha(0,0)(1+\lambda|E_{nr,ns}|^2)E_{nr,ns} + \alpha(r,s)(E_{(n+1)r,(n+1)_s} + E_{(n-1)r,(n-1)s}) + \lambda\alpha(r,s)(|E_{(n+1)r,(n+1)s}|^2 E_{(n+1)r,(n+1)s} + |E_{(n-1)r,(n-1)s}|^2 E_{(n-1)r,(n-1)s})]. \quad (1)$$

Here $\mathbf{d}=a(r\hat{i}+s\hat{j})$ for fixed integers r and s is the displacement vector between nearest-neighboring impurity containing cylinders along the waveguide channel, n runs over the integers, and $E_{nr,ns}$ is the electric field amplitude at the (nr,ns) waveguide channel site. The coupling coefficients $\alpha(0,0)$ and $\alpha(r,s)$ are determined from the periodic geometry and dielectric properties of the pure photonic crystal without waveguide channels, γ is a constant related to the dielectric properties of the cylinders forming the waveguide channel, and λ is a parameter characterizing the Kerr nonlinearity of the material in the waveguide channel. In particular, if $\lambda=0$ the material forming the waveguide is linear dielectric media, characterized by γ. For a detailed discussion of the relationships between the α's the γ, and the dielectric constants of the system, impurity medium, geometry, and electromagnetic Green's functions of the photonic crystal, see Refs. 5–9 and 25.

In this paper we are interested in the properties of the ILM solutions arising from generalizations of Eq. (1) to a number of topologically different systems. These are independent of the nature of the physical system being described and should be applicable to electromagnetic, phonon, and magnon systems characterized by equations of the form of Eq. (1) and its topological generalizations.

III. TRANSMISSION ANOMALIES IN WAVEGUIDES CONTAINING A BARRIER OF KERR NONLINEAR SITES

Consider a waveguide along the x-axis of a square lattice photonic crystal. The waveguide channel sites are labeled by

$(n,0)$ for n an integer. The propagation of energy in such a waveguide formed of a linear dielectric and containing a single barrier composed of a series of consecutive channel sites containing Kerr nonlinear dielectric material is studied. Energy in a traveling waveguide mode that is incident on the barrier from its left-hand side is reflected and transmitted through the barrier. During this process the incident wave interacts with bound modes within the barrier material, leading to a tunneling process in which the bound mode is an intermediate state assisting the transmission of energy through the barrier. This is the photonic crystal waveguide analogy of the reflection and transmission of light incident on a finite periodically layered Kerr nonlinear medium containing gap solitons.[26–28] The gap solitons are found to give rise to resonant anomalies in the transmission through the layered medium.[26–28] Such anomalies are also seen in transmission through the waveguide barrier.

The media of the waveguide channel is linear dielectric except for a barrier consisting of $2p+1$ consecutive waveguide channel sites [see Fig. 1(b)]. These sites are composed of Kerr nonlinear media and are labeled $(n,0)$ for $-p \leqslant n \leqslant p$. Outside this region, the channel sites $(n,0)$ for $n<-p$ or $n>p$ are formed of linear medium. The difference equations for this system are obtained by generalizing from Eq. (1) (Refs. 6,8) so that

$$E_{n,0} = \gamma_l[\alpha(0,0)E_{n,0} + \alpha(1,0)(E_{n-1,0} + E_{n+1,0})] \tag{2}$$

for $n \leqslant -p-2$ or $n \geqslant p+2$,

$$E_{\pm(p+1),0} = \gamma_l[\alpha(0,0)E_{\pm(p+1),0} + \alpha(1,0)E_{\pm(p+2),0}] + \gamma[\alpha(1,0)E_{\pm p,0} + \lambda\alpha(1,0)|E_{\pm p,0}|^2 E_{\pm p,0}], \tag{3}$$

$$E_{\pm p,0} = \gamma[\alpha(0,0)E_{\pm p,0} + \lambda\alpha(0,0)|E_{\pm p,0}|^2 E_{\pm p,0} + \alpha(1,0)E_{\pm(p-1),0} + \lambda\alpha(1,0)|E_{\pm(p-1),0}|^2 E_{\pm(p-1),0}] + \gamma_l\alpha(1,0)E_{\pm(p+1),0}, \tag{4}$$

and

$$E_{n,0} = \gamma[\alpha(0,0)E_{n,0} + \lambda\alpha(0,0)|E_{n,0}|^2 E_{n,0} + \alpha(1,0)(E_{n-1,0} + E_{n+1,0}) + \lambda\alpha(1,0)(|E_{n-1,0}|^2 E_{n-1,0} + |E_{n+1,0}|^2 E_{n+1,0})] \tag{5}$$

for $-p+1 \leqslant n \leqslant p-1$. In Eqs. (2)–(5) γ in the barrier may differ from γ_l of the linear sites, and the nonlinearity of the barrier is characterized by $\lambda \neq 0$.

In studying Eqs. (2)–(5) it is convenient to define $g = \gamma\alpha(0,0)$ and $g_l = \gamma_l\alpha(0,0)$. These parameters, respectively, measure the strength of the on site coupling in the Kerr dielectric and the linear waveguide channel. The ratio $b = \alpha(1,0)/\alpha(0,0)$ characterizes the relative strength of the nearest-neighbor to the on site coupling. In this notation, for example, Eq. (5) becomes $E_{n,0} = g[E_{n,0} + \lambda|E_{n,0}|^2 E_{n,0} + b(E_{n-1,0} + E_{n+1,0}) + \lambda b(|E_{n-1,0}|^2 E_{n-1,0} + |E_{n+1,0}|^2 E_{n+1,0})]$.

A solution of Eqs. (2)–(5) for electromagnetic waves incident on the barrier from the left is of the general form

$$E_{n,0} = ue^{ikn} + ve^{-ikn} \tag{6}$$

for $n<-p$,

$$E_{n,0} = xe^{ikn} \tag{7}$$

for $n>p$, and

$$E_{n,0} = a_n e^{i\theta_n} \tag{8}$$

for $-p \leqslant n \leqslant p$. Substituting into Eqs. (2)–(5) gives a set of equations that are solved essentially exactly for the transmission coefficient, $|x/u|^2$, at a fixed stop band frequency ω as a function of g for fixed λ. Within the portion of the waveguide channel made from linear media it is found that[8]

$$1 = g_l[1 + 2b\cos k] \tag{9}$$

so that g_l is simply related to b and the wave number, k, of the extended waveguide modes.

As an illustration, Eqs. (2)–(5) are evaluated using numerical values for the difference equations coupling constants for a particular model of a pure square lattice photonic crystal that was studied in Refs. 8 and 9. The pure photonic crystal used to generate these coefficients is based on a square lattice photonic crystal of dielectric cylinders with $R = 0.3779a_c$, $\epsilon_0 = 9$, surrounded by vacuum. A waveguide is introduced into the photonic crystal by replacing a complete row of cylinders along the x-axis by cylinders containing impurity material. The impurity material in each cylinder is centered on its axes, is of square cross section with sides oriented along the x- and y-axes, and has a cross-sectional area $S = (0.02a_c)^2$. For the waveguide to support modes at the stop gap frequency $\omega a_c/2\pi c = 0.440$ (a frequency at the center of one of the stop bands of the photonic crystal), it was shown in Refs. 8 and 9 that $b = 0.0869$. The value of b, for fixed ω, is the same for extended waves in waveguides made from linear media ($\lambda = 0$) as for ILM in waveguides made of Kerr media ($\lambda \neq 0$). In the linear portion of the waveguide Eq. (9) determines g_l needed to support a wave of wavenumber k in the channel at fixed b. This g_l sets the dielectric constant needed to support the incident, reflected and transmitted extended waveguide modes. In the Kerr nonlinear barrier, substituting Eqs. (6)–(8) in Eqs. (2)–(5) gives u and v in terms of k, λx^2, and g. Here g is related to the dielectric contrast in the Kerr portion of the waveguide channel.

To solve for the fields in the nonlinear barrier media, we proceed as follows. First, the values of k and b are fixed, and g_l is determined from Eq. (9). Next, the values of λ and x are fixed. Equations (2)–(5), then determine successively (a_p, θ_p) then (a_{p-1}, θ_{p-1}) and so on down to the end of the barrier media. The amplitudes u and v are solved for as the last of the successive solutions, and the transmission coefficient is computed. In the barrier media there is a region of solutions exhibiting optical bistability. In this region we have always chosen amongst the multiple field solutions so as to stay on the same branch of the transmission hysteresis curve. The solution outlined above parallels that commonly used to compute the optical transmission through a linear layered media.[36]

In Fig. 2 a plot is presented of the transmission through a barrier of five sites ($p=2$) versus g for a mode of frequency $\omega a_c/2\pi c = 0.440$ (i.e., $b = 0.0869$) and wave number $k = 2.5$. In this case the barrier does not display optical bistability. Results are shown for a number of values of the Kerr param-

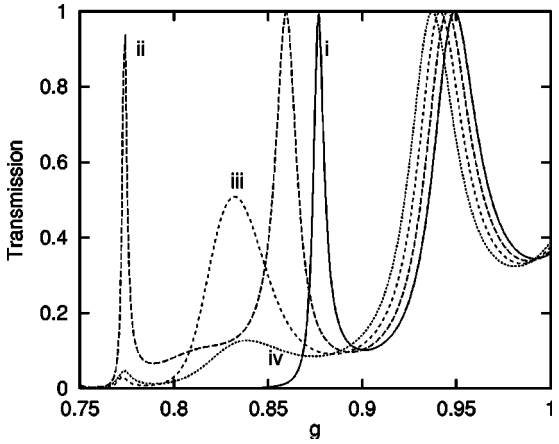

FIG. 2. Transmission coefficient for a barrier of 5 sites versus g (related to the dielectric contrast in the Kerr barrier) for an incident wave with $\omega a_c/2\pi c=0.440$ and $k=2.5$. Curves are shown for $\lambda x^2=0.0$, 0.00125, 0.0025, and 0.00375 labeled i, ii, iii, and iv, respectively.

eter such that $\lambda x^2=0.0$, 0.00125, 0.0025, or 0.00375 where x is the amplitude of the transmitted wave. The case $\lambda x^2=0.0$ corresponds to linear barrier media, and two resonances are observed in its transmission data one at $g=0.877$ and another at $g=0.949$. These are due to electromagnetic modes, bound to the barrier, that assist the incident electromagnetic energy in tunneling though the barrier. In the $\lambda x^2=0.00125$ case, these two peaks appear to shift to lower values $g=0.859$ and $g=0.945$ and a third peak appears at $g=0.774$. We shall see below that the appearance of the resonance in the $\lambda x^2=0.00125$ data at $g=0.774$ is related to an odd parity ILM. Increasing λx^2 to $\lambda x^2=0.0025$, the two upper peaks shift to lower values of $g=0.832$ and $g=0.941$ and the third (lowest) peak is greatly decreased. Some additional peaks, not found in the linear transmission data, are also observed off scale in the data. These are not of interest to us here. For $\lambda x^2=0.00375$ the two upper peaks are at $g=0.839$ and $g=0.937$, with the lower peak at $g=0.839$ greatly decreased in magnitude from its value at smaller λx^2. The third lowest peak is hardly seen. Through this series of increasing λx^2, it is interesting to consider the lower of the two upper transmission resonances. This occurs at $g=0.877$ for $\lambda x^2=0.0$, $g=0.859$ for $\lambda x^2=0.00125$, $g=0.832$ for $\lambda x^2=0.0025$, and $g=0.839$ for $\lambda x^2=0.00375$. The field intensity within the barrier at the maximum of these transmission resonances is closely related to that of the odd parity ILM in an infinite Kerr waveguide. This is also the case with the resonance that briefly occurs in the $\lambda x^2=0.00125$ system at $g=0.774$. In the following we shall concentrate our discussions on these two resonance peaks (the one arising from the $g=0.877$, $\lambda x^2=0.0$ resonance and the one arising from the $g=0.774$, $\lambda x^2=0.00125$ resonance) and show that they are related to odd parity ILM.

The discussion concerning these two peaks will proceed as follows: Both peaks are resonances in the transmission coefficient of the system. By solving for the field intensity distribution inside the nonlinear media in our transmission problem a comparison is made with the field distribution of the related ILM that would exist in an infinitely long Kerr waveguide characterized by the same parameters of dielectric constant, lattice parameter, Kerr parameter. For the two transmission peaks we treat, it will be found that the fields in the Kerr media at resonance transmission are almost identical to the fields of the ILM in the infinite Kerr waveguide. Furthermore, the ILM field distribution outside the Kerr media in our transmission problem would be very small. The bulk of the ILM field intensity is contained within the Kerr media in our transmission problem. The upper of the two resonance transmission peaks evolves from one of the resonance transmission peaks in the linear system (at $g=0.877$, $\lambda x^2=0.0$). As the Kerr nonlinearity becomes large enough it will be seen that the field distribution of the upper resonance approximates that of an ILM and the Kerr part of the dielectric develops into a field self-localizing trap, i.e., not only is the field distribution of the ILM observed in the barrier but the position dependent dielectric constant that self-localizes the ILM in the infinite Kerr system is reproduced in the Kerr barrier. In the case of the upper resonance the ILM fields are not as tightly localized as in the case of the lower of the two resonant peaks and the association with the ILM is less clear cut. It is an indication, however, that ILM can evolve from resonant modes of the linear system. The evolution of the upper of the two peaks from the linear resonance is slow and the fields in the Kerr barrier only begin to look ILM-like at large nonlinearities in which the dielectric constant is changed significantly by the field dependent Kerr contribution. For the upper peak the self-localizing effects of the Kerr contribution to the dielectric constant are never as great as they are for the lower of the two peaks. The lower of the two resonant peaks (at $g=0.0.774$, $\lambda x^2=0.00125$) is better characterized as an ILM resonance for two reasons:

(1) As the Kerr parameter is increased the transmission resonance is seen to suddenly appear and then just as suddenly disappear. This is a different behavior from that of the upper of the two resonant modes being discussed in this paragraph. It indicates that the resonance arises only from the self-localizing effects of the field distribution on the nonlinear dielectric constant of the system with no other assistance.

(2) The field intensities of the fields in the Kerr media at the lower resonance are essentially the same as the ILM in the infinite Kerr waveguide. Seeing that both of the transmission resonances treated here occur at waveguide parameters which sustain ILM and at resonance have the same field intensity distributions in the Kerr barrier as ILM in the infinite Kerr waveguides, we compare the maxima of the field intensities in the Kerr media to the intensities of the incident fields on the Kerr barrier. At resonance the fields inside the Kerr barrier are seen to be much larger than the intensity of the field of the waves incident on the barrier. For conditions off resonance this will no longer be the case. In fact, the field intensities in the Kerr media no longer are of the form of ILM but have very small field intensities. Rather than presenting numerous plots showing this, however, we prove this point by studying the ratio of the maximum field intensity in the barrier to the field intensity of the incident wave on the barrier at and near resonance. This then is the line of argument that we shall now give below. We shall first present the field intensities at resonance and then proceed in the order listed above with the rest of our arguments.

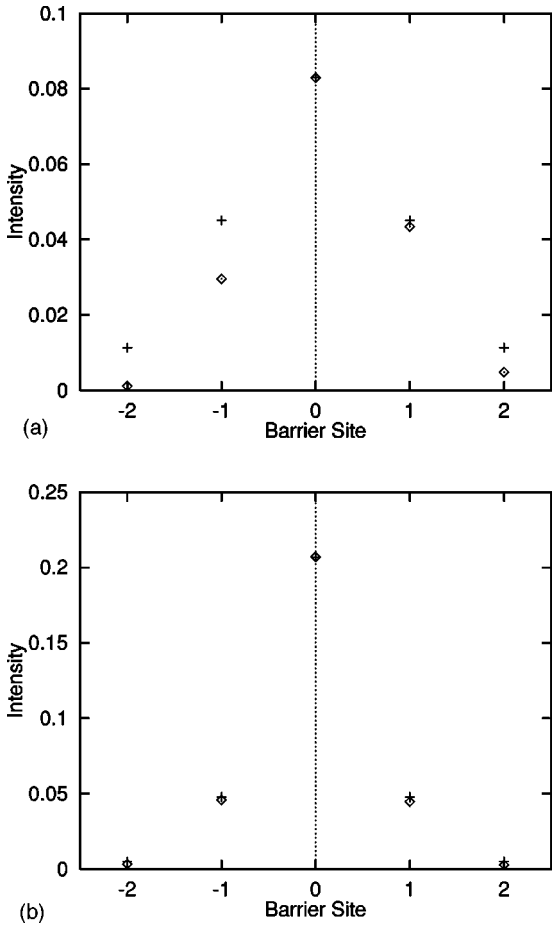

FIG. 3. Plot of $\lambda|E_{n,0}|^2$ versus n in the Kerr barrier of Fig. 2 for: (a) $g=0.832$, $\lambda x^2=0.0025$, (b) $g=0.774$, $\lambda x^2=0.00125$. The fields from the transmission data are indicated by diamonds and the fields from the infinite waveguide results in Ref. 8 are indicated by crosses. The fields in (b) cannot be distinguished on the scale of the plot.

In Fig. 3(a) a plot is given of $\lambda|E_{n,0}|^2$ versus n for the fields in the barrier of Kerr nonlinear medium at the $g=0.832$, $\lambda x^2=0.0025$ transmission maximum. The maximum field intensity in the Kerr medium is in the center ($n=0$) rod of the barrier and corresponds to $\lambda|E_{0,0}|^2=0.083$. Comparison of this field distribution is made with that of the odd parity ILM for $\lambda|E_{0,0}|^2=0.083$ in an infinite Kerr waveguide.[8] A reasonable agreement is found between the fields from the barrier transmission data and the ILM results. This indicates that the odd parity ILM is involved in the resonant transmission process. The theory in Ref. 8, however, gives $g=0.822$ as the value of g needed for an odd parity ILM with a maximum peak intensity $\lambda|E_{\text{maximum}}|^2=0.083$ to exist in the infinite Kerr waveguide. This differs from the value $g=0.832$ at the transmission maximum in the barrier transmission data. The discrepancy in the field distributions and g values between the barrier transmission anomaly and the ILM results from Ref. 8 accounts for the resonance transmission coefficient being less than one. The incident and transmitted field boundary conditions at the edges of the barrier do not allow for the generation of a field distribution in the nonlinear barrier that better simulates that of the ILM in an infinite Kerr waveguide. This is also observed in the asymmetry of the field intensity with respect to the center of the barrier. In nonlinear media the fields and dielectric constants determine each other self-consistently so that boundary conditions can be especially important in determining the fields in the nonlinear media. From the plot of $\lambda|E_{n,0}|^2$ it is seen that the nonlinearity from the Kerr term is large enough in this case to create a self-localizing contribution to the field dependent dielectric function, and the dielectric function in the barrier is essentially the same as that in the infinite Kerr waveguide supporting an ILM.

A stronger case for ILM resonant tunneling can be made for the transmission intensity maximum at $g=0.774$ in the $\lambda x^2=0.00125$ data. This does not appear to be related to either of the two resonances in the $\lambda x^2=0.0$ plot. In Fig. 3(b) the barrier field (exhibiting a field maximum $\lambda|E_{\text{maximum}}|^2=0.207$) is presented at this resonance and compared to odd parity ILM results with $\lambda|E_{\text{maximum}}|^2=0.207$ for the infinite Kerr waveguide.[8] In this case, the value of g for the ILM to exist in the infinite waveguide, from the theory of Ref. 8, is $g=0.772$. This is close to $g=0.774$ of the transmission data. In general the field profiles and g values of the transmission data and infinite waveguide results in Fig 3(b) are in much closer agreement than are those in Fig. 3(a). This indicates that an ILM is involved in the resonant scattering process in Fig. 3(b). In addition, from the plot of $\lambda|E_{n,0}|^2$ it is seen that the self-localization from the field dependent dielectric contribution is more evident than for the case in Fig. 3(a). That is why the resonance in Fig. 3(b) is a better example of resonant scattering from an ILM than is the one in Fig. 3(a). Again the dielectric function in the barrier essentially agrees with that found in an infinite Kerr waveguide supporting an ILM.

It is interesting to note that the barrier field intensities of Figs. 3 at the transmission resonances are very large compared to the intensities in the linear channels. (The fields in the Kerr nonlinear channel sites that are adjacent to channel sites formed from linear dielectric media are of the same order of magnitude as the fields in the linear media of the waveguide channels.) This can be seen from the peak intensities at the center of the barrier which fall off rapidly to the barrier edges. These intense field distributions at resonance are a general property associated with the resonant excitations of nonlinear modes in the barriers and junctions discussed in this paper. (The finite segment discussed in Sec. IV, due to its geometry, is an exception to this.) Another interesting property of the solutions of the difference equations is that changing $b>0$ for fixed λx^2 tends to shift the transmission peaks presented in Figs. 2 as functions of g along the g-axis but does not change their ordering along the g-axis or the general ILM nature of the barrier field intensity distribution. This has been checked for b that are roughly double those used in this paper. This is nice as the parameter in our theory which is most sensitive to the geometry of the waveguide channel is b.

As a further proof of the resonant nature of the transmission anomalies we have made a study of the ratio of the maximum field intensity in the Kerr barrier to the field intensity of the incident wave in the linear media of the incident channel. This is denoted $|E_{\text{max}}|^2/|u|^2$, where E_{max} is the

TABLE I. Barrier resonance and off-tuning study of $|E_{\max}|^2/|u|^2$.

Resonance	g	λx^2	$\lvert E_{\max}\rvert^2/\lvert u\rvert^2$	On or off resonance
	0.832	0.00125	6.5	off
Upper	0.832	0.00250	16.9	on
	0.832	0.00375	2.7	off
	0.815	0.00250	6.7	off
Upper	0.832	0.00250	16.9	on
	0.850	0.00250	6.1	off
	0.774	0.00000	1.7	off
Lower	0.774	0.00125	155.6	on
	0.774	0.00250	2.6	off
	0.764	0.00125	1.4	off
Lower	0.774	0.00125	155.6	on
	0.784	0.00125	10.3	off

maximum field intensity in the barrier and u is defined in Eq. (6). We have computed this ratio at resonance and then off tuned the parameters of the system from the resonance and observed the decrease in this ratio. Results of this study are presented in Table I. The two resonances occur at $g=0.832$, $\lambda x^2=0.0025$ and $g=0.774$, $\lambda x^2=0.00125$. In the table we first fix g and vary λx^2 about the resonance. This would correspond to varying the Kerr parameter or the field intensity of the time-dependent fields traveling in the waveguide. The decrease in $|E_{\max}|^2/|u|^2$ is most pronounced for the $g=0.0774$, $\lambda x^2=0.00125$ (lower resonance). Similarly, in a second set of variations λx^2 is fixed and g is varied about the resonance. (This could be accomplished experimentally by applying a time-independent uniform field to the Kerr material in the barrier region. This would give a uniform shift to g arising from the Kerr term in the dielectric.) The decrease in $|E_{\max}|^2/|u|^2$ is most pronounced for the $g=0.774$, $\lambda x^2=0.00125$ resonance. These results are in agreement with our view that the $g=0.774$, $\lambda x^2=0.00125$ resonance is the better example of an ILM transmission resonance. Similarly, off tuning effects are present in the upper resonance and for the other data in this paper. For brevity we shall limit the presentation of data on the off-tuning of the resonance to the waveguide barrier and the junction barrier treated in Sec. V. The other systems studied in this paper have similar resonance properties.

The results in Figs. 2 and 3 are for a system with $\lambda>0$. In this region of λ the system does not exhibit optical bistability. By changing the sign of λ in the parametrization of Figs. 2 and 3, a region of optical bistability is obtained. Figures 4 present results corresponding to those in Figs. 2 and 3 but for λ of opposite sign. Plots are shown for solutions lying on the upper branch of the bistable transmission coefficient curve. In Fig. 4(a) the transmission versus g for $\lambda x^2=-0.0025$ is presented and a transmission anomaly is observed at $g=0.8983$. The $g=0.8983$ peak corresponds to a resonant transmission assisted by an odd parity ILM with $\lambda|E_{\text{maximum}}|^2=-0.030$. To see this in Fig. 4(b) $-\lambda|E_{(n,0)}|^2$ versus n in the Kerr barrier is plotted for $g=0.8983$, $\lambda x^2=-0.0025$, and a comparison is made with results from Ref. 8 for odd parity ILM with $\lambda|E_{\text{maximum}}|^2=-0.030$ in the infinite Kerr waveguide. The Ref. 8 data for an infinite Kerr waveguide are in good agreement with data from the transmission study for the field intensity in the Kerr barrier. As with the discussion of the Fig. 3(a) data, the g needed to support the ILM in the infinite nonlinear waveguide differs from that found for the barrier transmission data. The theory in Ref. 8 requires $g=0.843$ for the ILM to exist in the infinite Kerr waveguide and the barrier resonance data gives a value $g=0.8983$. The discrepancy may be due to the finite size of the barrier. Again, off tuning the resonance greatly decrease the $|E_{\max}|^2/|u|^2$ ratio in the Kerr barrier and demonstrates that this is a true resonant scattering effect.

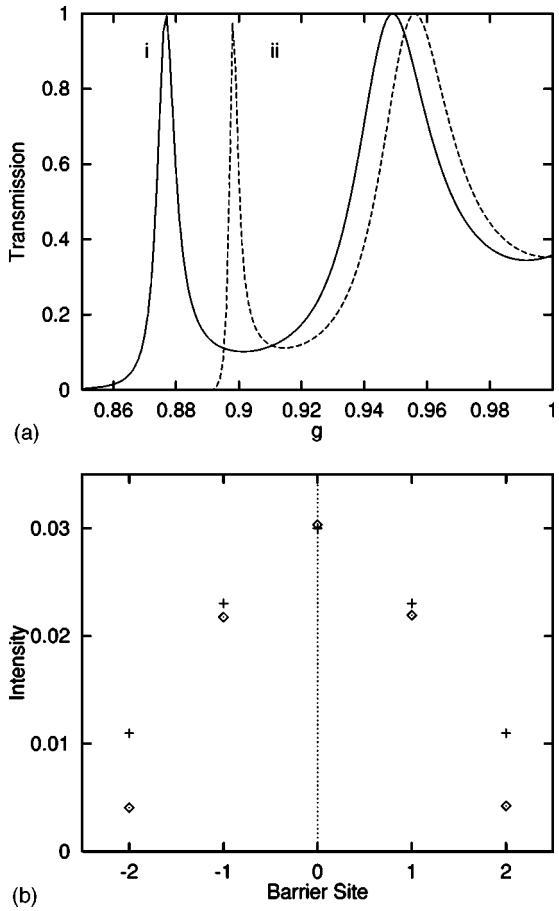

FIG. 4. (a) As in Fig. 2 but for $\omega a_c/2\pi c=0.440$ and $k=2.5$ with $\lambda x^2=0.0$ (labeled i) and $\lambda x^2=-0.0025$ (labeled ii). (b) Plot of $-\lambda|E_{n,0}|^2$ versus n in the Kerr barrier of Fig. 4(a) for $g=0.8983$ and $\lambda x^2=-0.0025$. The fields from the transmission data are indicated by diamonds and fields from the infinite waveguide results in Ref. 8 are indicated by crosses.

In Figs. 5 and 6 plots are presented, respectively, for the transmission coefficient and the barrier fields for a Kerr barrier of seven sites ($p=3$). These results are for a region in which there is no optical bistability. Figure 5(a) shows transmission coefficient results plotted versus g for $\lambda x^2=0.0$ and 0.00025. A fourth peak, not present in the linear data, is observed in the nonlinear data near $g=0.7914$. This peak is of significant amplitude only within the range $0.000125<\lambda x^2<0.000375$, and is associated with the pres-

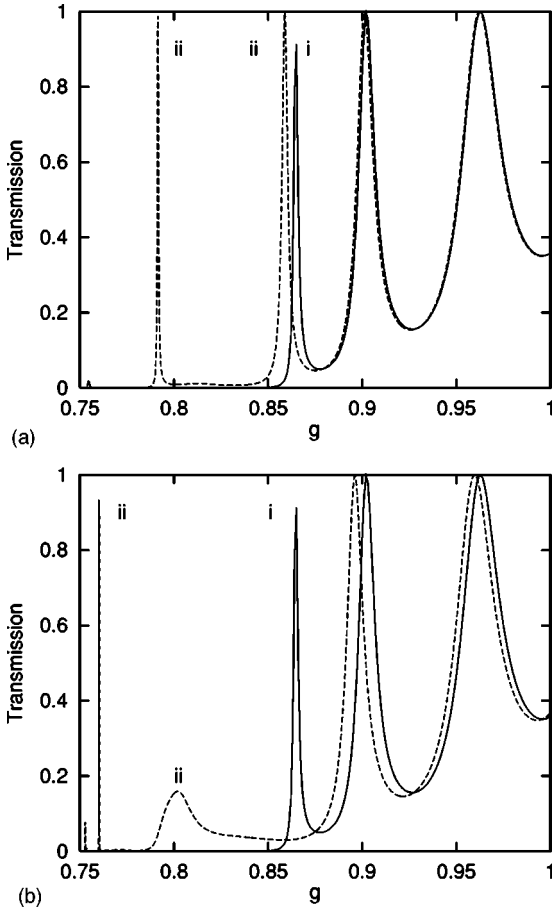

FIG. 5. Plots of the transmission coefficient for a barrier of seven Kerr sites versus g at $\omega a_c/2\pi c=0.440$ and $k=2.5$. In (a) results are shown for $\lambda x^2=0.0$ (labeled i) and 0.00025 (labeled ii). In (b) results are shown for $\lambda x^2=0.0$ (labeled i) and 0.0015 (labeled ii).

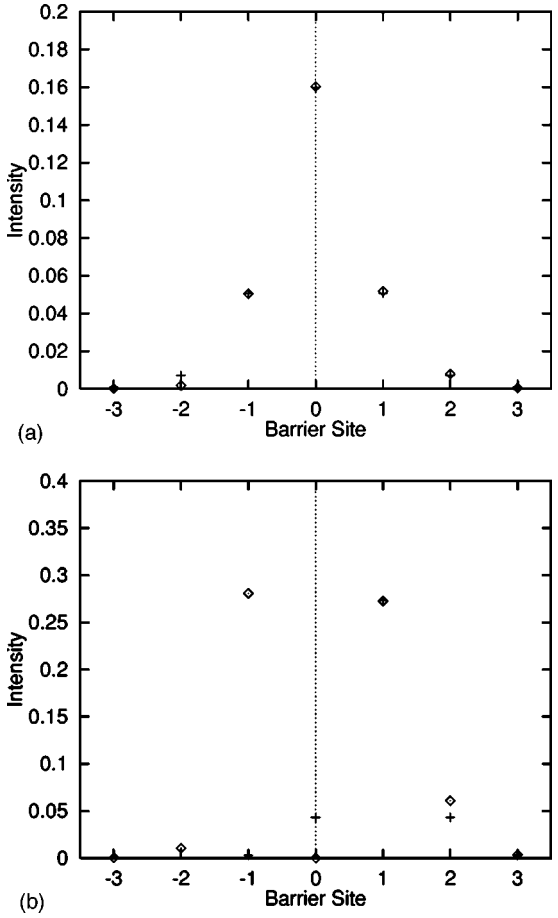

FIG. 6. Plots of $\lambda|E_{0,n}|^2$ versus n for the nonlinear barriers of seven sites sites considered in Fig. 5. Results are presented for: (a) $\lambda x^2=0.00025$ and $g=0.7914$ (diamonds) with a comparison made to odd parity ILM results from Ref. 8 (crosses), and (b) $\lambda x^2=0.0015$ and $g=0.7601$ (diamonds) with a comparison made to odd parity ILM results from Ref. 8 (crosses).

ence of an odd parity ILM in the Kerr barrier. In Fig. 5(b) transmission data plotted versus g is shown for $\lambda x^2=0.0$ and 0.0015. A fourth transmission peak at $g=0.7601$ is observed in the nonlinear data. It does not appear to be related to the two transmission peaks in the linear transmission, but from consideration of its field distribution in the barrier it is associated with a pair of odd parity ILM in the Kerr barrier. Figures 6 present $\lambda|E_{n,0}|^2$ versus n for the fields in the barrier at the fourth (lowest) resonance peaks in Figs. 5. A comparison of these field distributions is made with that of odd parity ILM field data of Ref. 8 for an infinite Kerr waveguide. In Fig. 6(a) the field distribution of the resonance at $\lambda x^2=0.00025$ and $g=0.7914$ is plotted and compared with the ILM data from Ref. 8 computed for $\lambda|E_{\text{maximum}}|^2=0.160$. (Note, the ILM exists in the infinite Kerr waveguide with this amplitude provided $g=0.7919$.) A reasonable agreement between the two sets of results is found, and this indicates that the ILM is involved in a resonant transmission process at this anomaly. In Fig. 6(b) the field distribution of the resonance at $\lambda x^2=0.0015$ and $g=0.7601$ is plotted. A comparison is made of the right peak in the field distribution data with ILM data from Ref. 8 computed for $\lambda|E_{\text{maximum}}|^2=0.273$. (For an ILM of this amplitude to exist in an infinite Kerr waveguide the theory of Ref. 8 requires $g=0.7435$.) It is seen that the ILM data from Ref. 8 would give a reasonable fit to each of the two peaks in the field distribution from the transmission data. As the two peaks both have fields that are distributed parallel in space, it appears the the tunneling in this case is due to a pair of odd parity ILM.

IV. TRANSMISSION ANOMALIES IN WAVEGUIDE PERPENDICULARLY BISECTING A KERR NONLINEAR SEGMENT

As an example of another system in which ILM can be resonantly excited, consider a infinite waveguide of linear media along the x-axis that perpendicularly bisects a finite segment of Kerr nonlinear waveguide channel oriented along the y-axis [see Fig. 1(c)]. Guided wave modes in the linear waveguide channel are reflected and transmitted in the linear waveguide channel as they interact with the Kerr segment. We will consider the calculation of the transmission and reflection coefficients of this scattering.

In this case the waveguide equations are given by

$$E_{n,0} = \gamma_l[\alpha(0,0)E_{n,0} + \alpha(1,0)(E_{n-1,0} + E_{n+1,0})] \quad (10)$$

for $|n|>1$,

$$E_{0,n} = \gamma[\alpha(0,0)E_{0,n} + \lambda\alpha(0,0)|E_{0,n}|^2E_{0,n} + \alpha(1,0)(E_{0,n-1} + E_{0,n+1}) + \lambda\alpha(1,0)(|E_{0,n-1}|^2E_{0,n-1} + |E_{0,n+1}|^2E_{0,n+1})] \quad (11)$$

for $p-1>|n|>0$,

$$E_{\pm1,0} = \gamma_l[\alpha(0,0)E_{\pm1,0} + \alpha(1,0)E_{\pm2,0}] + \gamma\alpha(1,0)[E_{0,0} + \lambda|E_{0,0}|^2E_{0,0}], \quad (12)$$

$$E_{0,0} = \gamma[\alpha(0,0)E_{0,0} + \lambda\alpha(0,0)|E_{0,0}|^2E_{0,0} + \alpha(1,0)(E_{0,1} + E_{0,-1})] + \gamma_l\alpha(1,0)(E_{-1,0} + E_{1,0}) + \gamma\lambda\alpha(1,0)[|E_{0,1}|^2E_{0,1} + |E_{0,-1}|^2E_{0,-1}], \quad (13)$$

$$E_{0,\pm p} = \gamma[\alpha(0,0)E_{0,\pm p} + \lambda\alpha(0,0)|E_{0,\pm p}|^2E_{0,\pm p} + \alpha(1,0)E_{0,\pm p\mp1} + \lambda\alpha(1,0)|E_{0,\pm p\mp1}|^2E_{0,\pm p\mp1}]. \quad (14)$$

A solution of this system is obtained by substituting

$$E_{n,0} = ue^{ikn} + ve^{-ikn} \quad (15)$$

for $n<0$,

$$E_{n,0} = xe^{ikn} \quad (16)$$

for $n>0$, and $E_{0,n}=a_n$ for $p\geqslant|n|$. Here Eq. (15) represents incident and reflected waves to the left of the Kerr segment, and Eq. (16) represents transmitted waves to the right of the Kerr segment. (Note, in the following calculations we impose the symmetry $a_n=a_{-n}$ on the segment modes. Other solutions with $a_n=-a_{-n}$ will not be considered.) This gives a system of nonlinear equations that are solved for the field amplitudes $\{u,v,a_n\}$ in terms of $g=\gamma\alpha(0,0)$, $b=\alpha(1,0)/\alpha(0,0)$, and λx^2.

In Fig. 7 results are shown, respectively, for the transmission coefficient versus $t=\lambda x^2$ and the fields in the segment versus position in the Kerr segment. In these plots $p=3$, $\omega a_c/2\pi c=0.440$, $b=0.0869$, $k=2.5$, and $g=0.772$. Figure 7(a) presents results for the transmission coefficient of the guided waves. The cusp in the transmission coefficient at $t=0.1584$ is associated with an odd parity ILM in the finite Kerr segment with $\lambda|E_{\text{maximum}}|^2=0.235$. To see this, in Fig. 7(b) a plot is given of the field intensity in the Kerr segment as a function of site label, n, for the $t=0.1584$ transmission data. A comparison is made with the fields, obtained from the theory of Ref. 8, of an odd parity ILM in an infinite Kerr waveguide with $\lambda|E_{\text{maximum}}|^2=0.235$. The g needed to sustain the ILM in the infinite waveguide is $g=0.760$ and this compares favorably with the $g=0.772$ of the resonant transmission data. The difference must come from the finite length of the Kerr segment of the transmission data.

The cusp in the transmission data at $t=0.1584$ corresponds to a maximum of the ratio $|E_{0,\pm1}/E_{0,0}|$ of the fields in the Kerr segment taken as a function of $t=\lambda x^2$. It appears that, at the $t=0.1584$ resonant excitation of the ILM, the fields in the Kerr segment broaden their spatial distribution. Off resonance (i.e., $t\neq0.1584$) the spatial distributions of the fields, centered about the (0, 0) site, in the segment are narrower. Equation (13) couples the waveguide modes to the $E_{0,\pm1}$ fields so that their broadening in the segment at the resonance shows up as a cusp in the transmission coefficient.

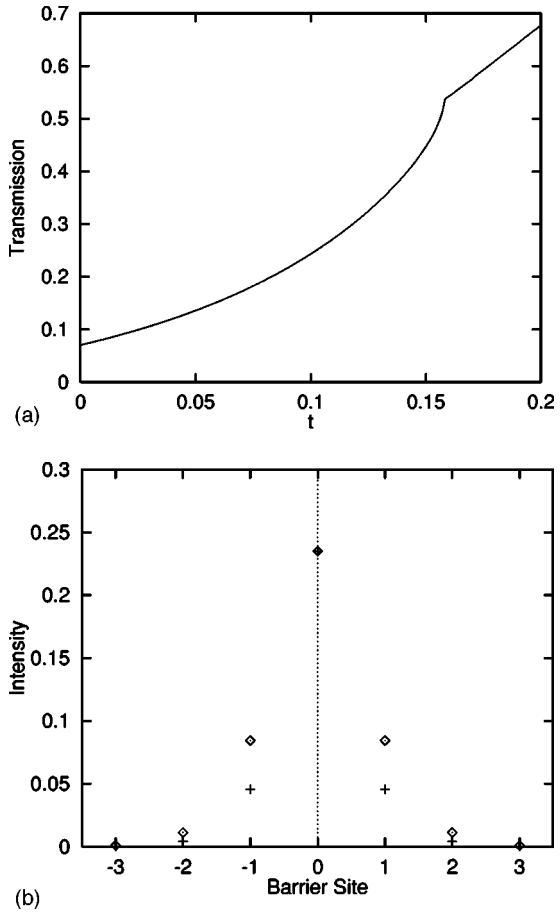

FIG. 7. Plot of (a) the transmission coefficient of the perpendicularly bisected nonlinear segment versus $t=\lambda x^2$ and (b) the field in the nonlinear segment versus n for the cusp at $t=0.1584$. In (b) the fields from the transmission data are given by diamonds and field from the ILM infinite Kerr waveguide results are given by crosses.

The observation of a cusp rather than a peak in the transmission is not unprecedented. In electron tunnel junction spectroscopy such resonant cusps are often found in the current versus voltage characteristics of the system.[30,31] They are observed in electronic tunnel junctions as anomalies in the higher derivatives of the current with respect to the voltage. The resonant transmission in our case follows from the observation of a transmission anomaly associated with the resonant excitation of an ILM mode in the target material. These are also the conditions that are counted in the observation of resonant transmissions in electron tunnel junction spectroscopy.[30,31]

V. TRANSMISSION ANOMALIES IN KERR NONLINEAR MEDIA JUNCTIONS

An infinite and a semi-infinite waveguide meet at a junction that forms a "T".[7] The infinite waveguide is along the

y-axis and the semi-infinite waveguide is along the positive *x*-axis [see Fig. 1(d)]. The media of the waveguide channels is linear dielectric except in the neighborhood of the junction vertex where the channels are Kerr nonlinear media. The nonlinear sites consist of the site at the center of the junction vertex and the p (where p is a positive integer) consecutive sites of each waveguide channel out from the vertex site.

The waveguides and their junction are characterized by a set of difference equations that are generalizations of Eqs. (1). For the semi-infinite channel along the *x*-axis,[7]

$$E_{nr,0} = \gamma_n \alpha(0,0)[1+\lambda_n |E_{nr,0}|^2]E_{nr,0} + \gamma_{n-1}\alpha(r,0)[1+\lambda_{n-1}|E_{(n-1)r,0}|^2]E_{(n-1)r,0} + \gamma_{n+1}\alpha(r,0)[1+\lambda_{n+1}|E_{(n+1)r,0}|^2]E_{(n+1)r,0}, \quad (17)$$

where $n=1,2,3,\cdots$. Here the Kerr parameters and γ_n characterizing the dielectric constants of the waveguide channel sites are defined by $\lambda_n=\lambda$ and $\gamma_n=\gamma$ if $|n|\leqslant p$ but $\lambda_n=0$ and $\gamma_n=\gamma_l$ if $|n|>p$. (Here we use the same notation for γ and γ_l of the Kerr and linear media sites as used in Sec. III and IV.) For the channel along the *y*- axis,

$$E_{0,nr} = \gamma_n \alpha(0,0)[1+\lambda_n |E_{0,nr}|^2]E_{0,nr} + \gamma_{n-1}\alpha(r,0)[1+\lambda_{n-1}|E_{0,(n-1)r}|^2]E_{0,(n-1)r} + \gamma_{n+1}\alpha(r,0)[1+\lambda_{n+1}|E_{0,(n+1)r}|^2]E_{0,(n+1)r}, \quad (18)$$

where $n=\pm 1,\pm 2,\pm 3,\cdots$, and at the junction of the two channels

$$E_{0,0} = \gamma_0 \alpha(0,0)[1+\lambda_0 |E_{0,0}|^2]E_{0,0} + \gamma_1\alpha(r,0)[E_{0,r}+E_{0,-r}+E_{r,0}] + \gamma_1\lambda_1\alpha(r,0)[|E_{0,r}|^2E_{0,r} + |E_{0,-r}|^2E_{0,-r} + |E_{r,0}|^2E_{r,0}]. \quad (19)$$

A solution to Eqs. (17)–(19) for a wave incident on the junction from the semi-infinite channel along the negative *y*-axis has the form

$$E_{n,0} = E_{0,n} = xe^{ikn} \quad (20)$$

for $n>p$,

$$E_{0,n} = ue^{ikn} + ve^{-ikn} \quad (21)$$

for $n<-p$,

$$E_{n,0} = b_n e^{i\phi_n} \quad (22)$$

for $0<n\leqslant p$, and

$$E_{0,n} = a_n e^{i\theta_n} \quad (23)$$

for $-p\leqslant n\leqslant p$. In the case studied here, the transmitted waves in the positive *x* and *y* channels are chosen to be of the same form. Substituting into Eqs. (17)–(19) gives the transmission coefficients at fixed stop band frequency ω (i.e., fixed $b=\alpha(1,0)/\alpha(0,0)$) as a function of γ for fixed λ.

The transmission coefficient, $2|x/u|^2$, is computed using similar methods to those used to study the barrier problem. Values of b and k are fixed and $g_l=\gamma_l\alpha(0,0)$ is obtained from Eq. (9). Specifying a value for λx^2, Eqs. (20)–(23) are substituted into Eqs. (17)–(19) and the resulting equations solved for u and v in terms of $g=\gamma\alpha(0,0)$, λx^2, and b. The solution proceeds by starting at the outgoing ends of the junction and working back along the difference equations through the junction to the end of the single incoming Kerr channel.

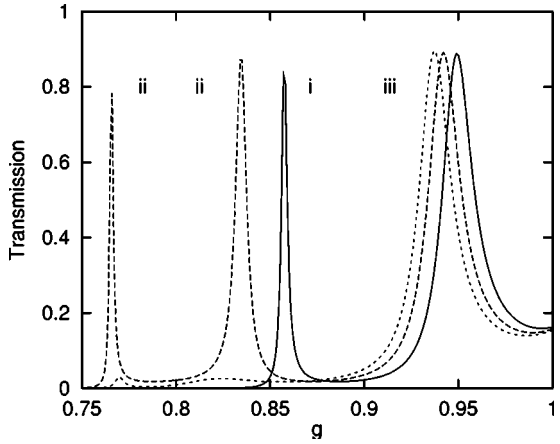

FIG. 8. Plots of the transmission coefficient for a junction with $p=2$ as a function of g for $\omega a_c/2\pi c=0.440$ and $k=2.7$. In this case there are one incident channel and two outgoing channels. Results are show for $\lambda x^2=0.0$, 0.00075, and 0.00125 which are labeled, respectively, i, ii, iii. A large third resonance peak is observed in the $g=0.00075$ data at $g=0.766$.

In Fig. 8 the transmission coefficient for a junction with $p=2$ is plotted vs g for $b=0.0869$ (i.e., $\omega a_c/2\pi c=0.440$), $k=2.7$ for various $\lambda x^2=0.0$, 0.00075, and 0.00125. The $\lambda x^2=0.00075$ data exhibits a third peak at $g=0.766$ that is not related to the peaks found in the $\lambda x^2=0.0$ and 0.00125 data. In Fig. 9 a plot is presented of the fields in the Kerr media of the junction as a function of the site indices for the $\lambda x^2=0.00075$ data at the $g=0.766$ resonance. (Note that the field amplitudes are the same in each of the outgoing junction channels.) A comparison plot is made of the ILM fields in an infinite waveguide made entirely of Kerr media.[7] The ILM solutions are from Ref. 7 for the case in which $\lambda|E_{0,0}|^2$

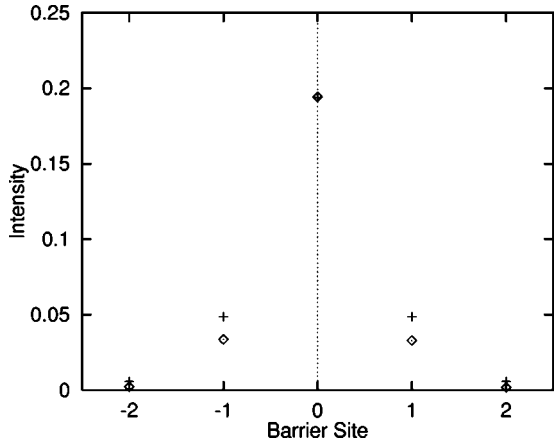

FIG. 9. Plots of $\lambda|E_{0,n}|^2$ (diamonds) for the junction transmission versus n at the $g=0.766$ resonance of the $\lambda x^2=0.00075$ data. For comparison, ILM results from Ref. 7 (crosses) for the junction of three semi-infinite Kerr nonlinear waveguides with $\lambda|E_{\text{maximum}}|^2=0.194$ are also shown.

TABLE II. Junction resonance $|E_{\max}|/|u|^2$ on and off resonance tuning.

g	λx^2	$\lvert E_{\max}\rvert^2/\lvert u\rvert^2$	On or off resonance
0.766	0.00050	0.70	off
0.766	0.00075	101.40	on
0.766	0.00100	0.32	off
0.760	0.00075	2.28	off
0.766	0.00075	101.40	on
0.770	0.00075	8.52	off

$=0.194$. The value of g needed to support the ILM in the infinite waveguide is from Ref. 7 given by $g=0.778$. This compares favorably with $g=0.766$ of the resonance in Fig. 8 and indicates that the transmission resonance is related to the excitation of an ILM in the nonlinear media of the junction.

A feeling for the distribution of the field intensities in the Kerr barrier at and off resonance can be obtained by computing the ratio of the maximum field intensity in the Kerr barrier to the field intensity of the incident wave on the barrier in the linear dielectric waveguide. In Table II these results are presented for the resonance at $(g=0.766, \lambda x^2 = 0.00075)$ and for a sequence of off tuned systems. The off tuning is done first by fixing $g=0.766$ and varying λx^2 about the resonance and then by fixing $\lambda x^2=0.00075$ and varying g about the resonance. It is found that: (1) The fields in the Kerr barrier at resonance can be much larger than the incident field intensity, and (2) small changes in λx^2 for fixed g or small changes in g for fixed λx^2 can quickly off tune the system from resonance. (Changes in λx^2 and g can be made as per our discussion of the Kerr barrier in Sec. III.) These effects are large at small changes in the system parameter for the junction resonance and give strong proof of the correctness of our association of the $g=0.766$, $\lambda x^2=0.00075$ resonance with the excitation of an ILM.

VI. CONCLUSIONS

The transmission properties of a number of different Kerr nonlinear targets within a system of linear dielectric photonic crystal waveguides have been studied. These include barriers, bisected barriers, and junctions. For these calculations, the frequency of the guided waves in the linear channels are fixed and the transmission through the targets are computed as a function of the dielectric constant of the target materials (g), the transmitted wave amplitude x, and the Kerr parameter (λ). Resonances are observed in the transmission data due to bound states in the barrier media. These occur in both linear and Kerr target materials. The Kerr targets in general exhibit more resonances than the linear media. Some of these are identified with ILM structures in infinite Kerr waveguides and junctions formed from three semi-infinite Kerr waveguide. The best correspondences with ILM solutions are made for systems with large $\lambda|E_{\text{maximum}}|^2$. This results in large changes of the target dielectric properties due to the Kerr nonlinearity. In such cases, the shape of the pulse is determined by the nonlinearity to a great extent, and the pulse is self localized by the dielectric profile it induces in the Kerr media.

Five interesting aspects of these transmission processes are: (1) Photonic crystal circuits offer a more topologically diverse set of targets exhibiting soliton related transmission resonances than do layered media. (2) The ILM-like solutions can be used to develop large field concentrations in the Kerr target materials. (Note: The field in the Kerr nonlinear channel sites that are adjacent to channel sites formed from linear dielectric media is of the same order of magnitude as the field in the linear media of the waveguide channels.) This may be of interest for applications. (3) The resonances observed in the transmission data of the nonlinear barriers and junctions can evolve, as the Kerr parameter increases from zero, from bound state resonances in the linear counterparts of these systems. Additional resonances are also found that do not originate from bound states in linear counterparts of the Kerr nonlinear barrier and junction systems. (4) The general features of the plot of the transmission coefficient versus g are determined to a great extent by λx^2. For fixed λx^2, the parameter b just scales the resonance peaks along the g-axis. (5) The transmission data offers an experimental method of observing ILM modes in a new type of optical system. The resonances arising from the ILM can be off tuned by varying the field intensities of the propagating waves in the waveguide channels or by the application of a uniform time-independent electric field to the Kerr media.

It is hoped that the results presented here will stimulate interest in nonlinear waveguides and circuits of waveguides in photonic crystals. The treatment involves a simple theory which can be quickly and easily solved for many circuit geometries. It provides initial ideas of what properties may exist in such systems. Recently, some experiments have measured intrinsic localized modes in nonoptical system,[25,33] and most recently in an array of optical waveguides.[34,35] Photonic crystal circuits offer a system in which to observed ILM optically. Just as optical gap solitons were predicted in optical layered media before they were originally observed experimentally (see Ref. 25 for a review of this work). It is hoped that the current work will lead to observation of ILM in photonic crystal circuits.

To conclude, we emphasize a few points upon which our presentation has been based. The resonances studied here are identified with ILM as: (1) They occur when the Kerr media barrier (finite junctions) satisfies conditions approximating those under which a system of infinite Kerr waveguides would support ILM excitations. (2) Off tuning the resonant conditions of the Kerr media of the barrier (finite junctions) so that the infinite Kerr systems would no longer support ILM turns off the transmission enhancement and changes the fields in the Kerr media of the barrier (finite junctions) so that they no longer resemble those of ILM. (3) At resonance the Kerr contributions to the dielectric constants in the Kerr barrier (junction) is a large self-localizing contribution approximating that found in infinite Kerr systems containing ILM. (4) At resonance the field intensities outside the Kerr barrier (junction) are small (i.e., replacing the linear dielectric media outside the barrier or junction with Kerr dielectric would be a small perturbation changing the resonant state to a bound state.). The results presented in this paper are for

small Kerr systems (small number of Kerr sites) and for small Kerr parameters, λ. We have chosen small systems in order to make the calculations easier. Nonlinear systems tend to be difficult to treat due to the great variety of complex behaviors they can exhibit. (This can be true for systems described by seemingly simple sets of nonlinear equations, e.g., remember the study of chaos. Remember, also, that even simple sets of nonlinear equations can display multiple solutions.) Beginning our search on a system with a small number of sites and for small nonlinearities allows us to more easily get a handle on classifying the behaviors exhibited. This, however, has limited us to the treatment of small pulse like excitations of the odd parity ILM type as these fit into the small Kerr barriers we have used. Nevertheless, it is known from our earlier would on ILM that odd parity ILM can occur as very narrow pulses so that we have had a high probability of observing these. Even parity ILM generally extend over a greater number of sites than do odd parity ILM are less probable to be found in small systems, and have not been observed in the treatment given here. As found in the work of Chen and Mills, large barriers can exhibit a complex behavior involving a variety of multiple pulses. In addition, the variety of multiple solutions can be a complication. We have chosen to limit the size of our system as we thought it useful in an initial presentation regarding single ILM pulses in a discrete nonlinear system.

ACKNOWLEDGMENTS

This work has been supported by the Army Research Office under Grant No. DAAD 19-01-1-0527. A.R.M. is grateful for support from the Department of Physics and Astronomy, Michigan State University where part of this work was done.

*Emai1 address: mcgurn@wmich.edu

[1] J. D. Joannopoulos, R. D. Meade, and J. N. Winn, *Photonic Crystals* (Princeton University Press, Princeton, 1995).
[2] J. D. Joannopoulos, P. R. Villeneuve, and S. Fan, Nature (London) **386**, 143 (1997).
[3] *Photonic Band Gaps and Localization*, edited by C. M. Soukoulis (Plenum, New York, 1992).
[4] *Photonic Band Gap Materials*, edited by C. M. Soukoulis (Kluwer, Dordrecht, 1996).
[5] A. R. McGurn, Phys. Rev. B **53**, 7059 (1996).
[6] A. R. McGurn, Phys. Rev. B **61**, 13235 (2000).
[7] A. R. McGurn, Phys. Rev. B **65**, 075406 (2002).
[8] A. R. McGurn, Phys. Lett. A **251**, 322 (1999).
[9] A. R. McGurn, Phys. Lett. A **260**, 314 (1999).
[10] S. F. Mingaleev, Y. S. Kivshar, and R. A. Sammut, Phys. Rev. E **62**, 5777 (2000).
[11] S. Mingalev and Y. Kivshar, Opt. Photonics News **13**, 48 (2002).
[12] N. Stefanou and A. Modinow, Phys. Rev. B **57**, 12127 (1998).
[13] A. Yariv, Y. Xu, R. K. Leei, and A. Scherer, Opt. Lett. **24**, 711 (1999).
[14] S. Mooherjea and A. Yariv, Opt. Express **9**, 91 (2001).
[15] A. J. Sievers and J. B. Page, in *Dynamical Properties of Solids*, edited by G. K. Horton and A. A. Maradudin (Elsevier, Amsterdam, 1995) Vol. 7, pp. 137–255.
[16] A. J. Sievers and S. Takeno, Phys. Rev. Lett. **61**, 970 (1989).
[17] S. Takeno and A. J. Sievers, Solid State Commun. **67**, 1023 (1988).
[18] A. J. Sievers and S. Takeno, Phys. Rev. B **39**, 3374 (1989).
[19] J. B. Page, Phys. Rev. B **41**, 7835 (1990).
[20] S. R. Bickham and A. J. Sievers, Phys. Rev. B **43**, 2339 (1991).
[21] S. R. Bickham, S. A. Kiselev, and A. J. Sievers, Phys. Rev. B **47**, 14206 (1993).
[22] S. A. Kiselev, S. R. Bickham, and A. J. Sievers, Phys. Rev. B **48**, 13508 (1993).
[23] S. A. Kieselv, S. R. Bickham, and A. J. Sievers, Phys. Lett. A **148**, 255 (1994).
[24] K. W. Sandusky and J. B. Page, Phys. Rev. B **50**, 866 (1994).
[25] A. R. McGurn, Chaos **13**, 754 (2003).
[26] D. L. Mills, *Nonlinear Optics: Basic Concepts* (Springer, New York, 1998).
[27] G. P. Agrawal, *Nonlinear Fiber Optics*, 2nd ed. (Academic, San Diego, 1995).
[28] W. Chen and D. L. Mills, Phys. Rev. Lett. **58**, 160 (1987).
[29] H. Freidrich, *Theoretical Atomic Physics* (Springer Verlag, Berlin, 1990).
[30] C. B. Duke, *Tunneling in Solids* (Academic, New York, 1969).
[31] H. Kuzmany, *Solid-State Spectroscopy: An Introduction* (Springer-Verlag, Berlin, 1998).
[32] R. Shimada, A. L. Yablonskii, S. G. Tikhodeev, and T. Ishihara, IEEE J. Quantum Electron. **38**, 872 (2002).
[33] M. Sato, B. E. Hubbard, A. J. Sievers, B. Luc, D. C. Zaplewski, and H. G. Craighead, Phys. Rev. Lett. **90**, 044102 (2003).
[34] D. Mandelik, H. S. Eisenberg, Y. Silberberg, R. Morandotti, and J. S. Aitchison, Phys. Rev. Lett. **90**, 253902 (2003).
[35] D. K. Campbell, S. Rlack, and Y. S. Kivshar, Phys. Today **57**, 43 (2004).
[36] P. Yeh, *Optical Waves in Layered Media* (Wiley, New York, 1988).